European Spine Journal
https://doi.org/10.1007/s00586-019-05901-w

ORIGINAL ARTICLE

GEORG SCHMORL PRIZE OF THE GERMAN SPINE SOCIETY (DWG) 2018: combined inflammatory and mechanical stress weakens the annulus fibrosus: evidences from a loaded bovine AF organ culture

Taryn Saggese[1] · Graciosa Q. Teixeira[1] · Kelly Wade[1] · Lydia Moll[1] · Anita Ignatius[1] · Hans-Joachim Wilke[1] · Raquel M. Goncalves[1,2,3,4] · Cornelia Neidlinger-Wilke[1]

Received: 3 August 2018 / Revised: 15 January 2019 / Accepted: 18 January 2019

Abstract

Purpose The pathomechanism of annulus fibrosus (AF) failure is still unknown. We hypothesise that mechanical overload and an inflammatory microenvironment contribute to AF structural weakening. Therefore, the objective of this study was to investigate the influence of these factors on the AF, particularly the translamellar bridging network (TLBN) which connects the AF lamellae.

Methods A bovine AF organ culture (AF-OC) model of standardised AF rings was used to study the individual and combined effects of cyclic tensile strain (CTS) and IL-1β (1 ng/mL) culture medium supplementation. AF-OCs were analysed for PGE_2 production (ELISA) and deposition of IL-6, COX-2, fibrillin, and MMP3 in the tissue (immunohistochemistry, IHC). The mechanical strength of the TLBN was evaluated using a peel test to measure the strength required to separate an AF segment along a lamellar bound.

Results The combination of CTS + IL-1β led to a significant increase in PGE_2 production compared to Control ($p < 0.01$). IHC evaluations showed that the CTS + IL-1β group exhibited higher production of COX-2 and MMP3 within the TLBN regions compared to the adjacent lamellae and a significant increase in IL-6 ratio compared to Control ($p < 0.05$). A significant decrease in the annular peel strength was observed in the CTS + IL1β group compared to Control ($p < 0.05$).

Conclusion Our findings suggest that CTS and IL-1β act synergistically to increase pro-inflammatory and catabolic molecules within the AF, particularly the TLBN, leading to a weakening of the tissue. This standardised model enables the investigation of AF/TLBN structure–function relationship and is a platform to test AF-focused therapeutics.

Graphical abstract

These slides can be retrieved under Electronic Supplementary Material.

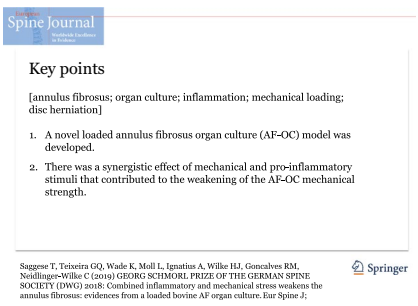

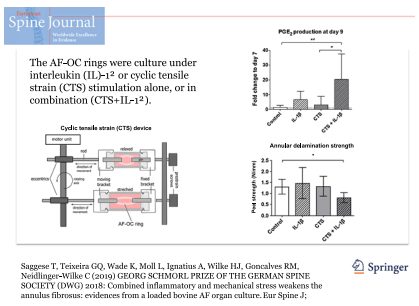

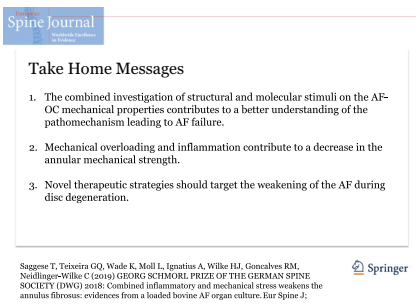

Keywords Annulus fibrosus · Organ culture · Inflammation · Mechanical loading · Disc herniation

Electronic supplementary material The online version of this article (https://doi.org/10.1007/s00586-019-05901-w) contains supplementary material, which is available to authorized users.

Extended author information available on the last page of the article

Published online: 28 January 2019

Introduction

Low back pain (LBP) is a recurrent occupational condition affecting up to 85% of the world population [1]. It is frequently linked to intervertebral disc (IVD) degeneration, prolapse or herniation, often requiring surgical interventions. Fissures and tears in the annulus fibrosus (AF) lamellae and endplate associated failure are considered to be the main causes of IVD prolapse [2]. With the loss of AF lamellae integrity, the inner nucleus pulposus (NP) soft tissue can extrude into the adjacent spinal canal, causing pain due to irritation of nerve roots [3, 4]. Currently, the pathomechanism leading to weakening of the AF structure and failure of the tissue integrity is not fully understood. Defects in the AF may arise from trauma, ageing or matrix degeneration, thereby compromising the AF structure, which becomes unable to withstand the hydrostatic pressure from the NP. Genetic predisposition [5] and physical overloading [6, 7], as well as inflammation factors [8], are known contributors to degenerative changes of the disc tissue. Nonetheless, it is not yet fully understood how these factors alter the structure and function of the AF tissue.

The AF is composed of concentric lamellae consisting primarily of collagen type I bundles. The orthogonal fibre orientation of the collagen alternates from lamella to lamella, thus providing very high resistance to tensile stresses which occur during disc bulging. These collagen-rich lamellae are separated by a thin proteoglycan-rich matrix, known as the interlamellar matrix (ILM). At intermittent locations, this ILM forms dense transverse bridges that cross the lamella before separating and reconnecting with the ILM. In this way, a three-dimensional elastic network named translamellar bridging network (TLBN), connecting the layers of the AF, is formed. This complex structure has been suggested to play an important role in preventing radial bulging of the disc under high axial loads [9, 10]. Biochemically, the TLBN consists of elastin, fibrillin, collagen type IV, aggrecan and other proteoglycans including versican and perlecan [11]. This proteoglycan-rich matrix has been proposed to allow the collagen bundles of the lamellae to slide over each other, preventing damage in extreme postures [12]. Additionally, the stiffness of the ILM is hypothesised to be central to the mechanical properties of the annular wall [13].

To date, few studies have investigated the functional role of the TLBN in the pathomechanism of disc degeneration [14]. Regarding a possible role of mechanical influences, Han et al. [14] studied strain distribution under optical coherence tomography (OCT) and reported significantly higher strains in the inter-/trans-lamellar matrix compared to the intralamellar regions. This uneven distribution of strain is proposed to make the TLBN more susceptible to mechanical damage or mechanobiology stimulation compared to the adjacent lamellae. However, little is known about how these mechanical or other factors influence matrix homoeostasis of the TLBN.

Disc degeneration involves the interaction of many factors, such as reduced nutrient supply, mechanical overloading, and levels of inflammatory molecules [15]. Increased disc matrix degradation has been observed in pro-inflammatory conditions [8, 16]. Inflammation is one of the key contributors to phenotype changes and apoptosis of disc cells. An increase in the presence of pro-inflammatory molecules has been described in degenerated and herniated IVD tissue, among which interleukin-1β (IL-1β) and tumour necrosis factor-α (TNF-α) are the most prominent [17]. During degeneration progression, many other cytokines and catabolic markers, such as prostaglandin E_2 (PGE_2), interleukins (IL-6, IL-8), nitric oxide, matrix metalloproteinases (MMPs), and MMPs with thrombospondin motifs (ADAMTS)-4 and -5, induce catabolic and inhibit anabolic matrix processes [8, 18].

To our knowledge, it has not been investigated whether interactions between mechanical loads and pro-inflammatory conditions influence the structural and functional integrity of the TLBN. Therefore, the objective of the present study is to investigate the influence of inflammatory and mechanical stress in a bovine AF organ culture (AF-OC) approach, which enables the application of defined cyclic tensile strain (CTS) under pro-inflammatory conditions. To investigate a possible interaction of both factors on the AF structure, cell viability, and production and distribution of TLBN matrix components were assessed. We hypothesise that matrix homoeostasis of the TLBN is altered by mechanical overload in presence of pro-inflammatory factors, thereby contributing to tissue structural weakening.

Methods

Tissue dissection and organ culture preparation

Bovine tails from animals aged 18–24 months were obtained from the local slaughterhouse (Fleischmarkt Donautal, Ulm). Caudal discs C2–3 to C6–7 were used for the organ culture model. Muscles and ligaments were removed to expose the IVDs; then the mid-region of each IVD was cut out using a custom-built cutting-tool, containing two parallel microtome blades 5 mm apart. Subsequently, to obtain AF tissue rings with consistent dimensions (5 mm height × 3 mm width), the IVDs were cut with a 20 or 22 mm metal punch (depending on IVD size). Then, the NP tissue was removed using a 14 or 16 mm punch, respectively. The AF rings were then cultured in IVD culture media, as previously described [19, 20]: low-glucose Dulbecco's Modified Eagle Medium (22320022, Gibco) supplemented

with 5% Foetal Bovine Serum Superior (S0615, Biochrom), 1% Penicillin–Streptomycin (10,000 U/mL-10,000 µg/mL, 15140122, Gibco), 0.5% Amphotericin B (250 µg/mL, 15290026, Gibco), 1% L-Glutamine (200 mM, 25030024, Gibco), 1% non-essential amino acids (K0293, Biochrom), and 1.5% of a 5 M NaCl/0.4 M KCl solution (to adjust osmolarity to 400 mOsm). The AF-organ cultures (AF-OCs) were maintained at 37 °C under 8.5% CO_2 and 6% O_2, for 7 days, with medium exchange every 2–3 days.

Organ culture stimulation with cyclic tensile strain and IL-1β

To investigate the effects of mechanical stimulation, a custom-made electro-mechanical device for application of CTS to deformable silicone dishes was used (Fig. 1a, b). The device developed by Neidlinger-Wilke et al. [21] was modified to include overhanging stainless steel pins in which the AF-OC rings could be hooked onto, and these were attached to the silicon dishes by a bracket. The eccentrics caused the pins to move 1 mm, generating a strain across the AF-OC rings of 9 ± 3%. This loading was applied cyclically at 1 Hz for 3 h per day for 5 days to generate a high physiological CTS range [22]. Recombinant human IL-1β (1 ng/mL, 201-LB, R&D) culture medium supplementation was used to promote pro-inflammatory conditions on the tissue. Four AF-OC rings from the same animal were separated into different groups, as described in the experimental scheme in Fig. 1. Briefly, AF-OCs were cultured under cyclic tensile strain (CTS), IL-1β culture medium supplementation, or both, CTS + IL-1β. Non-stimulated conditions were used as Control. Medium exchange was performed every 48 h, and samples were collected prior to each exchange. At the end of day 11, each AF-OC ring was divided into segments for histological and mechanical evaluations. For immunohistochemistry, a segment was fixed in 4% formalin for 72 h at 4 °C and then paraffin-embedded. For cell viability analysis, each segment was stained with ethidium homodimer-1 solution and then snap-frozen. For mechanical testing, segments were stored at − 80 °C.

Cell viability

To assess AF-OC viability, samples were rinsed in PBS, incubated at 37 °C in a 20 µM solution of ethidium homodimer-1 (EthD-1, E1169, Invitrogen) for 20 min, then washed twice with PBS (15 min each wash), and flash-frozen in liquid nitrogen and stored at − 80 °C. Cryosections of 10 µm were collected and stained with Hoechst and CF488A TUNEL apoptosis detection kit (30063, Biotium) according to the kit´s instructions. Cell viability was determined by fluorescence microscopy (Leica DMI6000B, Leica Microsystems), as:

$$\text{Cell viability (\%)} = \frac{\text{number of red stained cells} + \text{number of green stained cells}}{\text{number of blue stained cells}}$$

PGE_2 production

PGE_2 production was measured by enzyme-linked immunosorbent assay (ELISA), as per the manufacturer's instructions (K051, Arbor Assays). PGE_2 concentration at day 9 was normalised to day 7 (before transferring to silicone dishes) for each disc.

Immunohistochemistry

Localisation of TLBN structural proteins, matrix degradation enzymes and pro-inflammatory cytokines were assessed by avidin–biotin complex (PK-6100, Vector laboratories) immunohistochemistry (IHC) using NovaRED Peroxidase (HRP) Substrate Kit (SK-4800, Vector Laboratories). Sections with 10 µm thickness were cut from paraffin blocks and underwent citrate buffer antigen retrieval (pH 6.0, 85 °C, 20 min), followed by hyaluronidase (2 mg/mL in citrate buffer pH 8, 30 min, 37 °C) and collagenase (2 mg/mL in citrate buffer, pH 8, 30 min, 37 °C) digestion. For each marker, all samples were stained at the same time for comparison purposes. The antibodies and dilutions used are summarised in Table 1.

Microscopy and image analysis

IHC sections stained for IL-6, COX-2, fibrillin and MMP3 were imaged using bright-field and polarised light microscopy (Axiophot, Zeiss). Polarised light images were taken to identify the birefringent lamella matrix (LM) and the opaque/black TLBN regions, and the corresponding bright-field image was used to assess IHC staining (Fig. 2). Positive IHC staining was identified following colour deconvolution filter in Fiji Image processing software; NOVA red and haematoxylin colour channels were digitally separated, allowing quantification of colour intensity only in the NOVA red channel. Regions of interest were drawn around TLBN and adjacent LM areas; within each region, average pixel intensity was measured and the ratio (TLBN/LM) of staining intensity was calculated.

Mechanical testing

The strength of the TLBN matrix was evaluated using a peel test based on the methods established by Gregory et al. [23]. Briefly, rectangular AF segments were

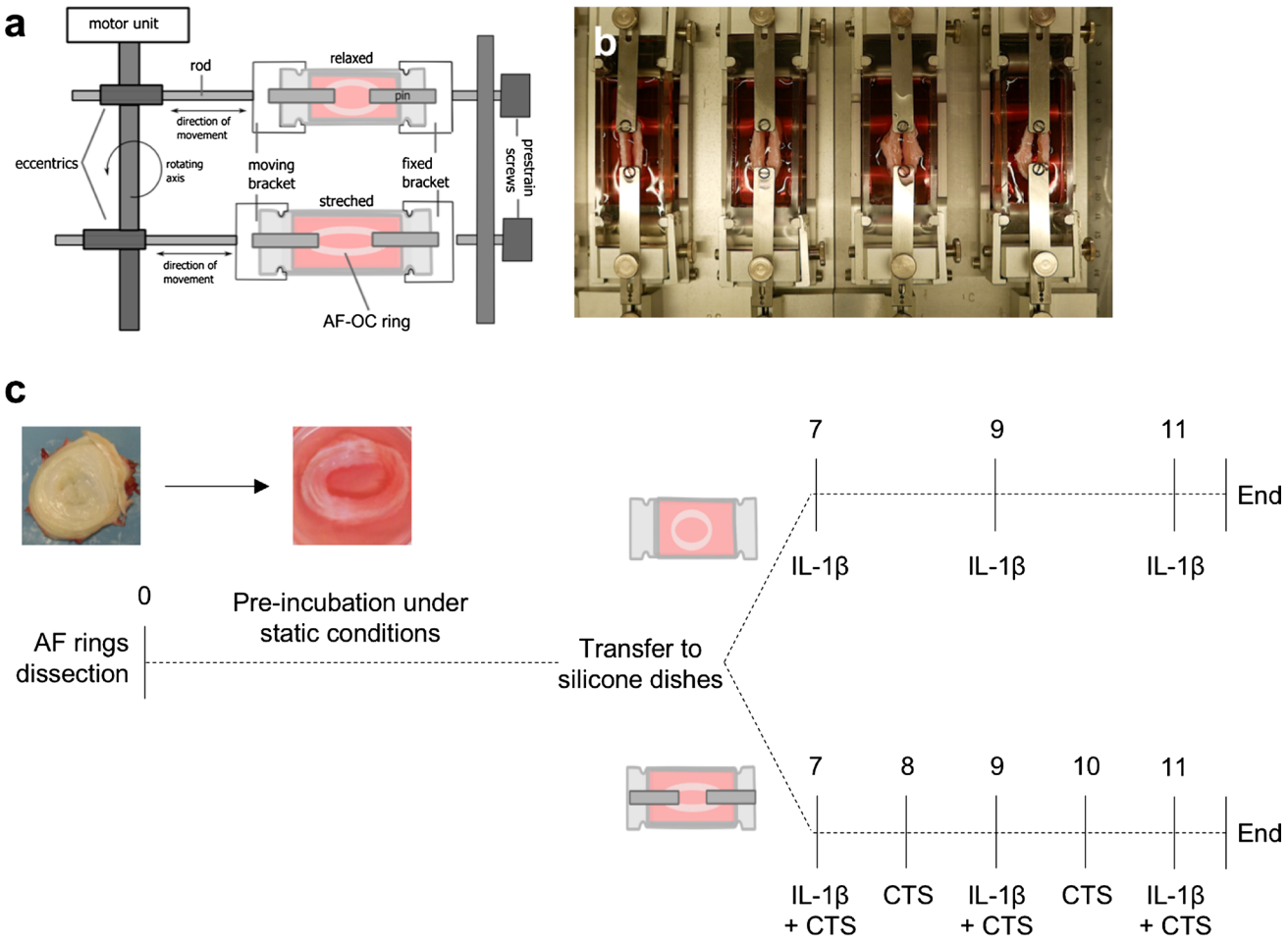

Fig. 1 Annulus fibrosus organ culture (AF-OC) preparation. Schematic representation of the custom-made electromechanical device for the application of cyclic tensile strain (CTS) to deformable silicone dishes (**a**) and the electromechanical device stretching the AF rings (**b**). Experimental timeline and experimental groups (**c**)

Table 1 Target molecules, antibodies and dilutions used for immunohistochemical evaluation

Target molecule	Antibody	Dilution
COX-2	Abcam: ab15191	1:200
Fibrillin-1	Thermo Fisher: MA5-12770	1:100
IL-6	Bioss: bs0782R	1:200
MMP3	Abcam: ab53015	1:200

dissected into a 'Y' configuration along a central lamella boundary. The sample was then clamped into a 'T' configuration in a uniaxial material testing machine and pulled apart at 0.5 mm/s, until complete separation of the sample. The average force in the plateau region of each force–displacement curve was used to calculate the delamination strength, according to Gregory et al. [23].

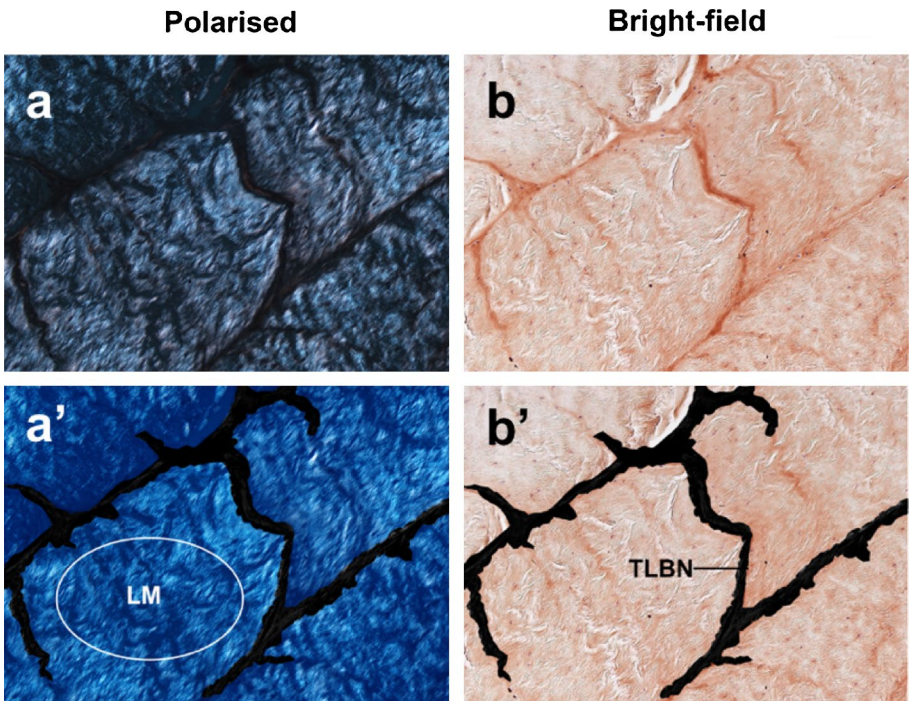

Fig. 2 Immunohistochemistry (IHC) quantification method. Polarised light images (**a**, **a′**) were used to define lamella matrix (LM) and translamellar bridging network (TLBN) regions of interest. Mean pixel intensity was measured in bright-field images (**b**, **b′**) for each region of interest to calculate TLBN/LM staining ratio

Statistical analyses

Results are presented as mean ± standard deviation. All statistical analyses were performed with GraphPad Prism 7. Data parametric distribution was analysed with D'Agostino–Pearson normality test. Nonparametric data were analysed using the Kruskal–Wallis test with Dunn's multiple comparison test to compare the different treatment groups. The two-way ANOVA with Tukey multiple comparison test was used to analyse the interaction between region and treatment for the IHC data.

Results

AF organ culture viability

Cell viability in all the AF-OC groups was above 80% after 11 days in culture. A small number of necrotic cells were present at the edges of the samples, and occasional TUNEL positivity (apoptotic cells) was seen within the tissue, namely in the CTS group (Fig. 3).

Production of inflammatory factors

PGE_2 release from stimulated AF-OC was quantified and compared between the different groups at day 9. Alone, IL-1β or CTS did not significantly increase PGE_2. However, in the presence of the combined treatment in the CTS + IL-1β group, PGE_2 release was significantly higher (about 20-fold increase, $*p < 0.01$) compared to the Control group (Fig. 4).

The distribution of COX-2 and IL-6 pro-inflammatory mediators in AF tissue and specifically in the TBLN was assessed by IHC at day 11 (Fig. 5). Polarised light microscopy enabled identification of the TLBN and LM regions within the transverse sections of AF. Since the lamella are composed of regularly arranged collagen fibrils, they are birefringent, and therefore are visibly bright, while the irregular matrix of the TLBN appears as opaque/black regions dividing the alternating lamellae. COX-2 was distributed all over the AF-OC tissue (Fig. 5a). A significant increase in its expression on the TBLN, in comparison to the LM, was observed for CTS + IL-1β group ($p < 0.05$, Fig. 5b). However, no significant differences were observed in the distribution of COX-2 in LM and TBLN regions or between the different treatment groups.

IL-6 deposition was detected in the LM and TLBN of samples from all groups (Fig. 5a). For Control, IL-1β and CTS single groups, IL-6 was similarly distributed within both regions, while in the CTS + IL-1β treatment, the production of IL-6 was significantly higher in the TLBN compared to the adjacent LM, and this ration was significantly higher than in the Control group ($p < 0.05$, Fig. 5b). This indicates that only the TLBN region was affected by the

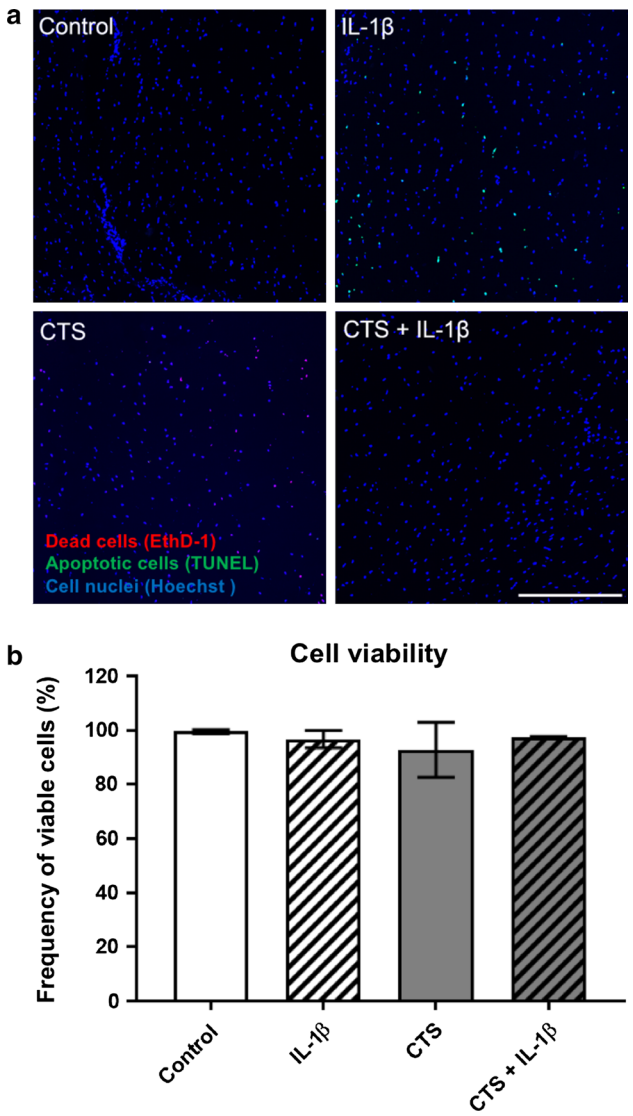

Fig. 3 Representative fluorescence microscopy images of TUNEL staining (**a**). Dead cells (red, EthD-1), apoptotic cells (green, TUNEL) and Hoechst counterstain of cell nuclei (blue) in Control, CTS, IL-1β and CTS + IL-1β groups (scale bar, 500 µm). Cell viability (**b**) presented as frequency of viable cells (%). Data are shown as mean ± standard deviation, $n = 5$

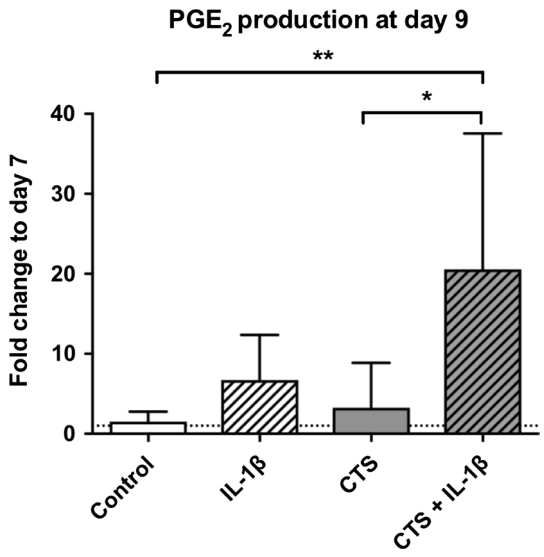

Fig. 4 Prostaglandin E_2 released to the supernatant by AF cells cultures in basal or degenerative conditions at day 9 relative to day 7. Data are shown as mean ± standard deviation, $n = 7$, $^{*}p < 0.05$; $^{**}p < 0.01$

combined treatment. Two-way ANOVA analysis found a significant interaction of region and treatment ($p < 0.05$, Table 2).

ECM remodelling

The ECM remodelling of AF-OCs was evaluated by fibrillin and MMP3 IHC (Fig. 6). Fibrillin staining was dense and dark in the TLBN, and weak and diffuse in the LM (Fig. 6a). Although no significant differences in the fibrillin deposition were detected between the different stimuli, a significantly higher staining intensity in the TLBN of samples from Control and IL-1β groups ($p < 0.05$) was found. MMP3 was expressed in both cells and matrix throughout the tissue. Significantly higher staining intensity was detected in the TLBN regions (compared to adjacent LM) of CTS + IL-1β group ($p < 0.05$, Fig. 5c). Using two-way ANOVA analysis, significant staining intensity differences were observed between the TLBN and LM regions for both fibrillin and MMP3 ($p < 0.001$), but not between the different treatments (Table 2).

Mechanical properties

At the end of the experiment, a biomechanical peel-test was performed in AF-OC tissue segments (Fig. 7a–c). Force–displacement curves showed an initial increase in force, then a plateau phase (Supplementary Fig. S1). Particularly in the Control, IL-1β and CTS groups, the plateau region was interrupted by steep peaks and troughs, while the CTS + IL-1β curves seemed to be smoother. Therefore, the mean force along one or more plateau regions was used to calculate the average annular delamination strength for a given sample. Interestingly, the CTS + IL-1β group was found to have a 40% lower delamination strength compared to the Control group ($p < 0.05$, Fig. 7d).

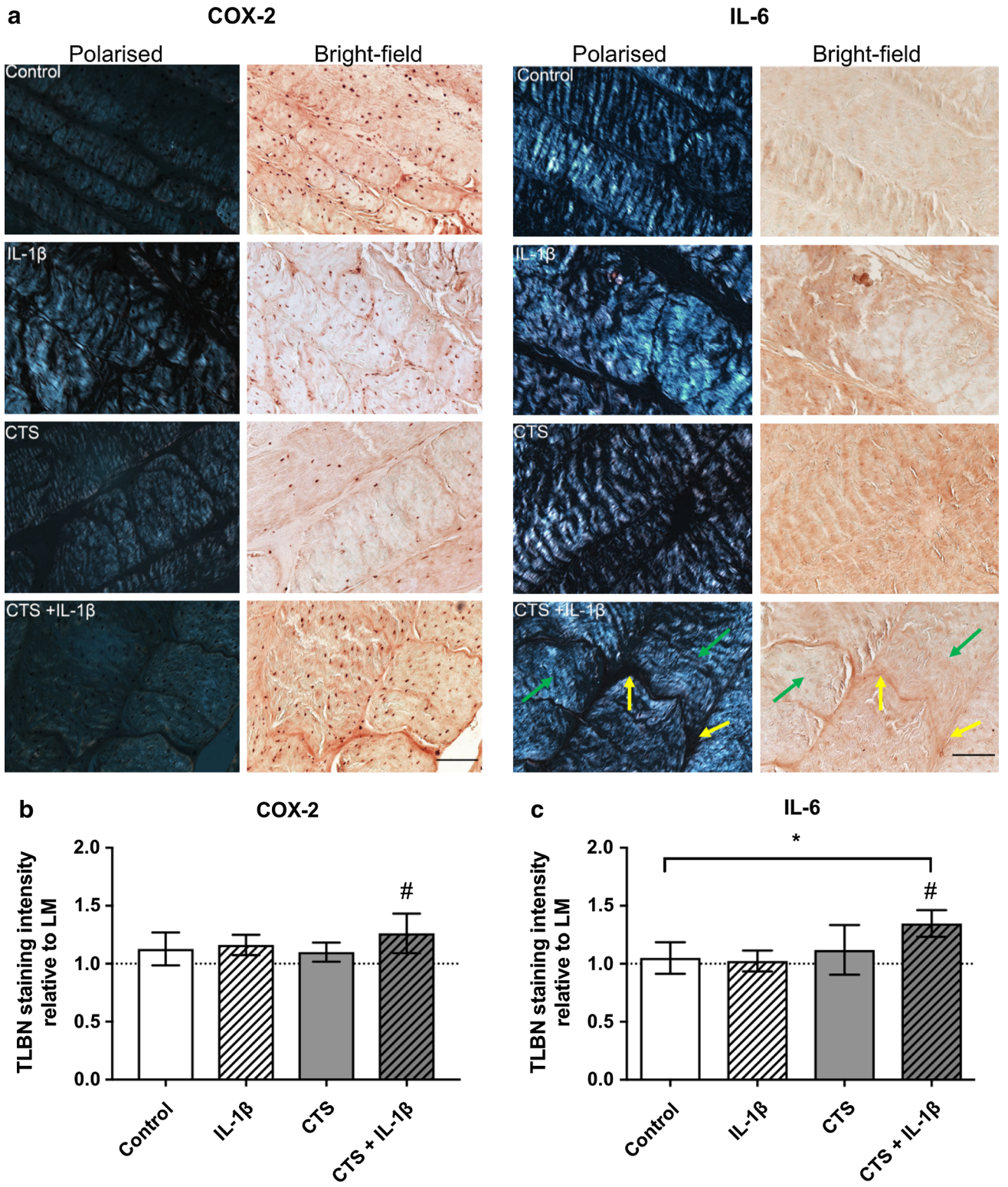

Fig. 5 Pro-inflammatory factors produced by AF cells cultures in basal or degenerative conditions, at day 11. Representative images (**a**) under polarised light and bright-field of COX-2 and IL-6 distribution within the translamellar bridging network (TLBN, *yellow arrows*) and the lamella matrix (LM, *green arrows*) of AF organ cultures; *scale bar*, 200 µm. COX-2 (**b**) and IL-6 (**c**) staining intensity in the TLBM relative to LM. Data are shown as mean ± standard deviation, $n = 5$; *significant effect of treatment, $^{*}p < 0.05$; $^{\#}$ significant effect of region, $^{\#}p < 0.05$

Table 2 Two-way ANOVA results from analysis of immunohistochemical staining of the AF-OC tissues

Source of variation	Region	Treatment	Interaction	
COX-2	**	ns	ns	
IL-6	*	ns	*	CTS + IL-1β
MMP3	***	ns	ns	
Fibrillin	***	ns	ns	

Discussion

In this study, a suitable AF-OC model was developed to investigate the AF structure–function relationship by stimulation with mechanical overloading in a pro-inflammatory environment. IL-1β is a well-characterised pro-inflammatory cytokine, previously shown to stimulate inflammation in IVD cells at concentrations ranging from 1 to 100 ng/mL [19, 24, 25]. Here, 1 ng/mL IL-1β was used to simulate a mild inflammatory environment. Interestingly, at this dose, IL-1β alone seemed to have no significant effect on any of the parameters analysed.

Although disc herniations may not be symptomatic or spontaneously regress, in many patients it may lead to chronic low back pain. There are few clinical solutions that target the underlying cause of disc degeneration [26–28], and new therapies that promote IVD regeneration and/or control inflammation-associated pain are needed. The question of how inflammation together with mechanical stress influence IVD herniation remains controversial, and given the lack of adequate models, we have developed this bovine AF-OC to address with a special focus the differences in annular tissue weakening between TLBN and LM. Although they cannot mimic the complexity of in vivo trials, these explant cultures present several advantages in comparison to in vitro studies, since they recreate a more physiologically relevant environment of disc degeneration compared to mechanical stimulation of IVD cells [29]. The bovine caudal discs are a well-accepted biological and biomechanical model for human discs which is easily available and has a similar cellular composition to human discs [30, 31].

Mechanical loading is crucial to mimic IVD physiological conditions. Previous in vitro studies found a complex cellular response to cyclic tensile strain in AF cells [32, 33]. CTS was shown to induce catabolic or anabolic factors and to modulate/upregulate inflammatory factors depending on strain magnitude, frequency and duration [33, 34]. In an in vitro study of the combined effects of IL-1β and CTS, Miyamoto et al. [35] reported that higher doses of inflammatory factors (10 ng/mL IL-1β) or higher magnitudes of mechanical loading (20% CTS) alone could induce PGE_2 production by both AF and NP cells, with the stimuli combination producing a strong synergistic response. In the present study, we showed that 1 ng/mL IL-1β or 9% CTS alone did not significantly increase PGE_2 release by the AF cells, but the combination of these stimuli did produce a strong synergistic response, resulting in a significant increase in PGE_2.

Additionally, these combined stimuli increased IL-6 and COX-2 production in the TBLN region compared to the LM. While IL-6 staining increase was significant in comparison to the unstimulated controls, COX-2 expression did not present statistically significant differences. This discrepancy might be explained by the fact that PGE_2 is also produced by COX-1 in human chondrocytes [36], or differences in COX-2/PGE_2 kinetics which contribute to the observed findings in our AF-OC model [37]. More recently, TNF-α stimulation of a whole IVD organ culture together with degenerative mechanical loading resulted in decreased anabolic and increased pro-inflammatory gene expression in both the AF and NP tissues [38]. Interestingly, Lang et al. [38] found an increase in IL-6 gene expression within the NP but not the AF region in response to inflammation and mechanical loading. This finding taken together with the increase in IL-6 protein expression seen only within the TLBN in our study could suggest that the proteoglycan-rich TLBN responds to the combined stimuli in a manner more similar to NP than to AF tissue.

Due to the interwoven nature of the TLBN through the lamella of the AF, separation of these regions for cell isolation and RNA extraction is not easy to perform. Consequently, previous TLBN studies have focused on histologically characterising the structural matrix components as identifying the TLBN as proteoglycan-rich. Our study adds to these findings the identification of a significantly higher expression of the catabolic enzyme MMP3 in the TLBN compared to the lamella matrix. Together, the IHC findings suggest that the TLBN is more affected by the combined stresses than the lamellae of AF. Therefore, it seems that a region-specific pro-inflammatory cascade leads to matrix breakdown and tissue weakening.

In the first study investigating the role of the TLBN in disc degeneration, Gregory et al. [39] induced disc degeneration in an in vivo model by injury and showed a resultant 30% decrease in delamination strength 3 months post-operatively. However, no mechanism for the findings was proposed. In the present study, we found that a mild inflammatory environment in combination with mechanical loading led to an upregulation of IL-6 coupled with a 40% decrease in delamination strength after 5 days of stimulation. These findings suggest that the initiation of a region-specific pro-inflammatory cascade leads to matrix breakdown and tissue weakening. While we did not find a significant decrease in fibrillin expression in response to the combined treatment, the TLBN matrix consists of many different components [11] and a decrease in any of

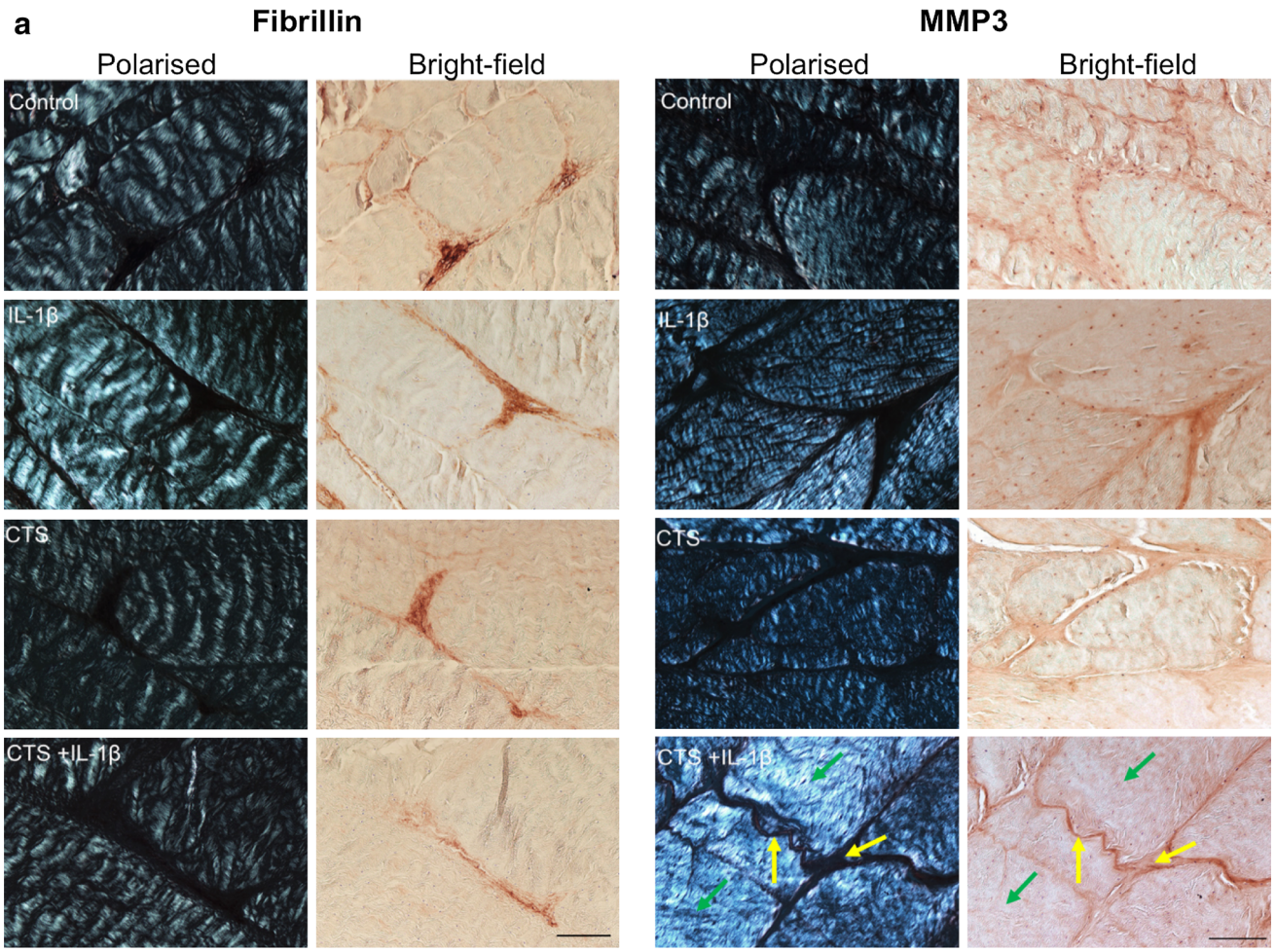

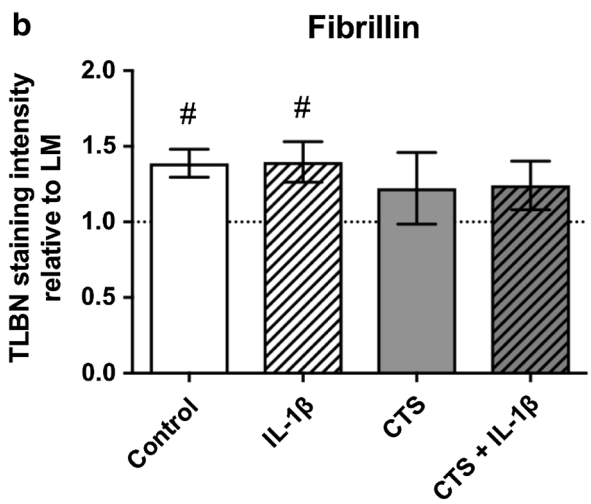

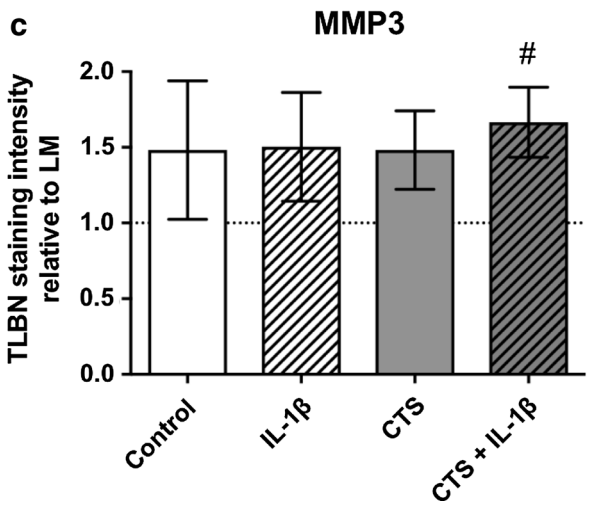

Fig. 6 Matrix composition of the AF rings cultured in basal or degenerative conditions, at day 11. Representative images (**a**) under polarised light and bright-field of fibrillin and MMP3 distribution within the translamellar bridging network (TLBN, *yellow arrows*) and the lamellae (LM, *green arrows*) of AF organ cultures; *scale bar*, 200 µm. Fibrillin (**b**) and MMP3 (**c**) staining intensity in the TLBM relative to LM. Data are shown as mean ± standard deviation, $n = 5$; $^{\#}$significant effect of region, $^{\#}p < 0.05$

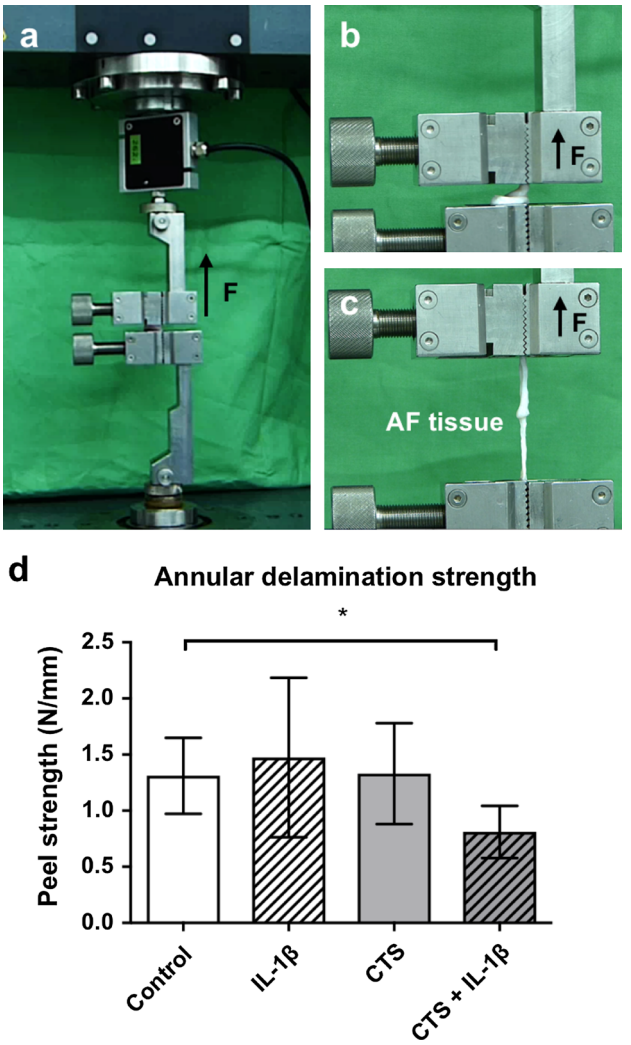

Fig. 7 Set-up of the material properties testing of AF tissue (**a**), after 11 days in culture under different stimuli, with half an AF ring clamped at the tabs into a 'T' configuration in the uniaxial material testing machine (*arrows* indicate the movement direction of the upper arm). Detailed look on the AF segment being pulled apart (at 0.5 mm/s) into a 'Y' configuration along a lamella boundary (**b**, **c**). Annular delamination strength as function of displacement rate (N/mm) for all conditions tested (**d**). Data are shown as mean ± standard deviation, $n = 6$, $^{*}p < 0.05$

these could be responsible for the observed decrease in delamination strength. Future studies concerning gene expression specifically of the TLBN region should be conducted, potentially by using laser capture microdissection technology. Moreover, future work will focus on the translation of these findings to human tissue, by investigating changes in human AF samples from patients suffering from different disc pathologies, namely disc herniation (versus healthy donors), and identifying the distribution of different inflammation and degeneration markers between the TLBN and the adjacent tissue (LM regions).

Conclusion

The novel AF-OC model presented in this study demonstrates how mechanical loading and a pro-inflammatory microenvironment may particularly affect the TLBN and integrity of the annular wall, without the need for a complex whole IVD organ culture system. Additionally, it was shown that the synergistic interaction of IL-1β and mechanical overload resulted in increased expression of PGE_2 and IL-6, the latter specifically within the TLBN, but not in the lamellae of the AF. This synergic action was also shown to decrease the annular mechanical strength. Overall, these results provide novel insights into the mechanism of how a degenerating disc can lead to tissue weakening and annular wall failure. Our findings show that small changes in the homoeostasis of the TLBN are capable of significantly weakening the tissue, highlighting the importance of the development of strategies to specifically target the weakening of this structure during disc degeneration.

Acknowledgements The authors of the present study wish to thank the local certified abattoir Fleischmarkt Donautal for kindly providing to us the bovine tails. We wish to thank Mrs. Iris Baum, Mrs. Patrizia Horny, Mrs. Marion Tomo, Mrs. Anna Weigl, Mrs. Anastasia Raiber, Mr. Zhiyao Yong and Mr. Alexander Vogel for the excellent support. We also acknowledge the German Spine Foundation (*Deutsche Wirbelsäulenstitung*), the German Academic Exchange Service (DAAD), the *Conselho de Reitores das Universidades Portuguesas,* the Ulm University (L.SBN.0157) and the Alexander von Humboldt Foundation for their financial support. The funding agencies did not have any involvement in the study design, data collection/analysis/interpretation, manuscript preparation or in the decision to submit the manuscript for publication.

Compliance with ethical standards

Conflict of interest All authors declare that they have no conflict of interest.

Ethical approval This study did not involve animal experiments or any studies with human participants performed by any of the authors. The bovine tails were obtained from cattle which were slaughtered for alimentary purposes.

References

1. Hoy D, Bain C, Williams G, March L, Brooks P, Blyth F, Woolf A, Vos T, Buchbinder R (2012) A systematic review of the global prevalence of low back pain. Arthritis Rheum 64:2028–2037. https://doi.org/10.1002/art.34347
2. Rajasekaran S, Bajaj N, Tubaki V, Kanna RM, Shetty AP (2013) ISSLS Prize winner: the anatomy of failure in lumbar disc herniation: an in vivo, multimodal, prospective study of 181 subjects. Spine 38:1491–1500. https://doi.org/10.1097/BRS.0b013e31829a6fa6

3. Adams MA, Dolan P (2012) Intervertebral disc degeneration: evidence for two distinct phenotypes. J Anat 221:497–506. https://doi.org/10.1111/j.1469-7580.2012.01551.x
4. Stefanakis M, Luo J, Pollintine P, Dolan P, Adams MA (2014) ISSLS Prize winner: mechanical influences in progressive intervertebral disc degeneration. Spine 39:1365–1372. https://doi.org/10.1097/BRS.0000000000000389
5. Battie MC, Videman T, Levalahti E, Gill K, Kaprio J (2007) Heritability of low back pain and the role of disc degeneration. Pain 131:272–280. https://doi.org/10.1016/j.pain.2007.01.010
6. Adams MA, Freeman BJ, Morrison HP, Nelson IW, Dolan P (2000) Mechanical initiation of intervertebral disc degeneration. Spine 25:1625–1636. https://doi.org/10.1097/00007632-200007010-00005
7. Lotz JC, Chin JR (2000) Intervertebral disc cell death is dependent on the magnitude and duration of spinal loading. Spine 25:1477–1483. https://doi.org/10.1097/00007632-200006150-00005
8. Risbud MV, Shapiro IM (2014) Role of cytokines in intervertebral disc degeneration: pain and disc content. Nat Rev Rheumatol 10:44–56. https://doi.org/10.1038/nrrheum.2013.160
9. Yu J, Schollum ML, Wade KR, Broom ND, Urban JP (2015) ISSLS Prize Winner: a detailed examination of the elastic network leads to a new understanding of annulus fibrosus organization. Spine 40:1149–1157. https://doi.org/10.1097/BRS.0000000000000943
10. Yu J, Winlove PC, Roberts S, Urban JP (2002) Elastic fibre organization in the intervertebral discs of the bovine tail. J Anat 201:465–475. https://doi.org/10.1046/j.1469-7580.2002.00111.x
11. Melrose J, Smith SM, Appleyard RC, Little CB (2008) Aggrecan, versican and type VI collagen are components of annular translamellar crossbridges in the intervertebral disc. Eur Spine J 17:314–324. https://doi.org/10.1007/s00586-007-0538-0
12. Schollum ML, Appleyard RC, Little CB, Melrose J (2010) A detailed microscopic examination of alterations in normal annular structure induced by mechanical destabilization in an ovine model of disc degeneration. Spine 35:1965–1973. https://doi.org/10.1097/BRS.0b013e3181e0f085
13. Mengoni M, Luxmoore BJ, Wijayathunga VN, Jones AC, Broom ND, Wilcox RK (2015) Derivation of inter-lamellar behaviour of the intervertebral disc annulus. J Mech Behav Biomed Mater 48:164–172. https://doi.org/10.1016/j.jmbbm.2015.03.028
14. Han SK, Chen CW, Labus KM, Puttlitz CM, Chen Y, Hsieh AH (2016) Optical coherence tomographic elastography reveals mesoscale shear strain inhomogeneities in the annulus fibrosus. Spine 41:E770–E777. https://doi.org/10.1097/BRS.0000000000001463
15. Vergroesen PP, Kingma I, Emanuel KS, Hoogendoorn RJ, Welting TJ, van Royen BJ, van Dieen JH, Smit TH (2015) Mechanics and biology in intervertebral disc degeneration: a vicious circle. Osteoarthr Cartil 23:1057–1070. https://doi.org/10.1016/j.joca.2015.03.028
16. Molinos M, Almeida CR, Caldeira J, Cunha C, Goncalves RM, Barbosa MA (2015) Inflammation in intervertebral disc degeneration and regeneration. J R Soc Interface 12:20141191. https://doi.org/10.1098/rsif.2014.1191
17. Le Maitre CL, Hoyland JA, Freemont AJ (2007) Catabolic cytokine expression in degenerate and herniated human intervertebral discs: IL-1beta and TNFalpha expression profile. Arthritis Res Ther 9:R77. https://doi.org/10.1186/ar2275
18. Le Maitre CL, Freemont AJ, Hoyland JA (2005) The role of interleukin-1 in the pathogenesis of human intervertebral disc degeneration. Arthritis Res Ther 7:R732–R745. https://doi.org/10.1186/ar1732
19. Teixeira GQ, Boldt A, Nagl I, Pereira CL, Benz K, Wilke HJ, Ignatius A, Barbosa MA, Goncalves RM, Neidlinger-Wilke C (2016) A degenerative/proinflammatory intervertebral disc organ culture: an ex vivo model for anti-inflammatory drug and cell therapy. Tissue Eng C Methods 22:8–19. https://doi.org/10.1089/ten.tec.2015.0195
20. Neidlinger-Wilke C, Mietsch A, Rinkler C, Wilke HJ, Ignatius A, Urban J (2012) Interactions of environmental conditions and mechanical loads have influence on matrix turnover by nucleus pulposus cells. J Orthop Res 30:112–121. https://doi.org/10.1002/jor.21481
21. Neidlinger-Wilke C, Wilke HJ, Claes L (1994) Cyclic stretching of human osteoblasts affects proliferation and metabolism: a new experimental method and its application. J Orthop Res 12:70–78. https://doi.org/10.1002/jor.1100120109
22. Stokes IA (1987) Surface strain on human intervertebral discs. J Orthop Res 5:348–355. https://doi.org/10.1002/jor.1100050306
23. Gregory DE, Bae WC, Sah RL, Masuda K (2012) Anular delamination strength of human lumbar intervertebral disc. Eur Spine J 21:1716–1723. https://doi.org/10.1007/s00586-012-2308-x
24. Shen B, Melrose J, Ghosh P, Taylor F (2003) Induction of matrix metalloproteinase-2 and -3 activity in ovine nucleus pulposus cells grown in three-dimensional agarose gel culture by interleukin-1beta: a potential pathway of disc degeneration. Eur Spine J 12:66–75. https://doi.org/10.1007/s00586-002-0454-2
25. Cho H, Lee S, Park SH, Huang J, Hasty KA, Kim SJ (2013) Synergistic effect of combined growth factors in porcine intervertebral disc degeneration. Connect Tissue Res 54:181–186. https://doi.org/10.3109/03008207.2013.775258
26. Sakai D, Schol J (2017) Cell therapy for intervertebral disc repair: clinical perspective. J Orthop Translat 9:8–18. https://doi.org/10.1016/j.jot.2017.02.002
27. Vadalà G, Russo F, Di Martino A, Denaro V (2015) Intervertebral disc regeneration: from the degenerative cascade to molecular therapy and tissue engineering. J Tissue Eng Regen Med 9:679–690. https://doi.org/10.1002/term.1719
28. Masuda K (2008) Biological repair of the degenerated intervertebral disc by the injection of growth factors. Eur Spine J 17(Suppl 4):441–451. https://doi.org/10.1007/s00586-008-0749-z
29. Wuertz K, Urban JP, Klasen J, Ignatius A, Wilke HJ, Claes L, Neidlinger-Wilke C (2007) Influence of extracellular osmolarity and mechanical stimulation on gene expression of intervertebral disc cells. J Orthop Res 25:1513–1522. https://doi.org/10.1002/jor.20436
30. Alini M, Eisenstein SM, Ito K, Little C, Kettler AA, Masuda K, Melrose J, Ralphs J, Stokes I, Wilke HJ (2008) Are animal models useful for studying human disc disorders/degeneration? Eur Spine J 17:2–19. https://doi.org/10.1007/s00586-007-0414-y
31. Horner HA, Roberts S, Bielby RC, Menage J, Evans H, Urban JP (2002) Cells from different regions of the intervertebral disc: effect of culture system on matrix expression and cell phenotype. Spine 27:1018–1028. https://doi.org/10.1097/00007632-200205150-00004
32. Sowa G, Agarwal S (2008) Cyclic tensile stress exerts a protective effect on intervertebral disc cells. Am J Phys Med Rehabil 87:537–544. https://doi.org/10.1097/PHM.0b013e31816197ee
33. Sowa G, Coelho P, Vo N, Bedison R, Chiao A, Davies C, Studer R, Kang J (2011) Determination of annulus fibrosus cell response to tensile strain as a function of duration, magnitude, and frequency. J Orthop Res 29:1275–1283. https://doi.org/10.1002/jor.21388
34. Gilbert HT, Hoyland JA, Freemont AJ, Millward-Sadler SJ (2011) The involvement of interleukin-1 and interleukin-4 in the response of human annulus fibrosus cells to cyclic tensile strain: an altered mechanotransduction pathway with degeneration. Arthritis Res Ther 13:R8. https://doi.org/10.1186/ar3229
35. Miyamoto H, Doita M, Nishida K, Yamamoto T, Sumi M, Kurosaka M (2006) Effects of cyclic mechanical stress on the production of inflammatory agents by nucleus pulposus and anulus fibrosus derived cells in vitro. Spine 31:4–9. https://doi.org/10.1097/01.brs.0000192682.87267.2a

36. Mastbergen SC, Jansen NW, Bijlsma JW, Lafeber FP (2006) Differential direct effects of cyclo-oxygenase-1/2 inhibition on proteoglycan turnover of human osteoarthritic cartilage: an in vitro study. Arthritis Res Ther 8:R2. https://doi.org/10.1186/ar1846
37. Chan MM, Moore AR (2010) Resolution of inflammation in murine autoimmune arthritis is disrupted by cyclooxygenase-2 inhibition and restored by prostaglandin E2-mediated lipoxin A4 production. J Immunol 184:6418–6426. https://doi.org/10.4049/jimmunol.0903816
38. Lang G, Liu Y, Geries J, Zhou Z, Kubosch D, Sudkamp N, Richards RG, Alini M, Grad S, Li Z (2018) An intervertebral disc whole organ culture system to investigate proinflammatory and degenerative disc disease condition. J Tissue Eng Regen Med 12:e2051–e2061. https://doi.org/10.1002/term.2636
39. Gregory DE, Bae WC, Sah RL, Masuda K (2014) Disc degeneration reduces the delamination strength of the annulus fibrosus in the rabbit annular disc puncture model. Spine J 14:1265–1271. https://doi.org/10.1016/j.spinee.2013.07.489

Affiliations

Taryn Saggese[1] · Graciosa Q. Teixeira[1] · Kelly Wade[1] · Lydia Moll[1] · Anita Ignatius[1] · Hans-Joachim Wilke[1] · Raquel M. Goncalves[1,2,3,4] · Cornelia Neidlinger-Wilke[1]

✉ Cornelia Neidlinger-Wilke
cornelia.neidlinger-wilke@uni-ulm.de

[1] Institute of Orthopaedic Research and Biomechanics, Trauma Research Centre, Ulm University, Helmholtzstraße 14, 89081 Ulm, Germany

[2] Instituto de Investigação e Inovação em Saúde (i3S), Universidade do Porto, R. Alfredo Allen, 4200-135 Porto, Portugal

[3] Instituto de Engenharia Biomédica (INEB), Universidade do Porto, R. Alfredo Allen, 4200-135 Porto, Portugal

[4] Instituto de Ciências Biomédicas Abel Salazar (ICBAS), Universidade do Porto, R. Jorge de Viterbo Ferreira 228, 4050-313 Porto, Portugal